Sequential recognition of discrete export signals in flagellar subunits during bacterial Type III secretion

Authors

Owain J. Bryant[a] , Paraminder Dhillon[a], Colin Hughes[a], Gillian M. Fraser[a,*]

Affiliations

[a]Department of Pathology, University of Cambridge, Tennis Court Road, Cambridge, CB2 1QP, United Kingdom

Corresponding author

[*]Gillian M. Fraser

Department of Pathology, University of Cambridge, Tennis Court Road, Cambridge, CB2 1QP, United Kingdom

Phone: +44 1223 330245

Email: gmf25@cam.ac.uk

Keywords

Type III secretion system; protein export; bacterial flagella biogenesis

[b]Owain Bryant current address: Department of Biochemistry, University of Oxford, South Parks Road, Oxford, OX1 3QU

[c]Paraminder Dhillon current address: The FEBS Journal Editorial Office, 59 St Andrew's House, Cambridge, CB2 3BZ, United Kingdom

Abstract

The flagellar T3SS delivers proteins from the bacterial cytosol to nascent cell surface flagella. Early subunits of the flagellar rod and hook are unchaperoned and contain their own export signals. One export signal, the gate recognition motif (GRM) docks subunits at the export gate, which must then open for unfolded subunits to enter the flagellar channel. Here, we identify a second signal at the extreme N-terminus of flagellar rod/hook subunits and determine that key to the signal is its hydrophobicity. We show that the two export signals are recognised sequentially, with the N-terminal signal being recognised only after subunits have docked at the export gate. The position of the N-terminal signal relative to the GRM is important, as a FlgD deletion variant (FlgDshort), in which the distance between the N-terminal signal and the GRM was shortened, stalled at the export machinery and was not exported. The attenuation of motility caused by FlgDshort was suppressed by mutations that destabilised the closed conformation of the FlhAB-FliPQR flagellar export gate, suggesting that the hydrophobic N-terminal signal might trigger gate opening.

Introduction

Type III Secretion Systems (T3SS) are multi-component molecular machines that deliver protein cargo from the bacterial cytosol either to their site of assembly in cell surface flagella or virulence factor injectosomes, or directly to their site of action in eukaryotic target cells or the extracellular environment [1-5]. The flagellar T3SS (fT3SS) directs the export of thousands of structural subunits required for the assembly and operation of flagella, rotary nanomotors for cell motility that extend from the bacterial cell surface [1],[6]. Newly synthesised subunits of the flagellar rod,

hook and filament are targeted to the fT3SS, where they are unfolded and translocated across the cell membrane, powered by the proton motive force and ATP hydrolysis, into an external export channel that spans the length of the nascent flagellum [7],[8]. During flagellum biogenesis, when the rod/hook structure reaches its mature length, the fT3SS switches export specificity from recognition of 'early' rod/hook subunits to 'late' subunits for filament assembly [9],[10]. This means that early and late flagellar subunits must be differentiated by the fT3SS machinery to ensure that they are exported at the correct stage of flagellum biogenesis. This is achieved, in part, by targeting subunits to the export machinery at the right time using a combination of export signals in the subunit mRNA and/or polypeptide. T3SS substrates contain N-terminal signals for targeting to the export machinery, however these signals do not share a common peptide sequence [11-15]. In addition, some substrates are piloted to the T3SS machinery by specific chaperones [16-21].

The core export components of the fT3SS are evolutionarily related to those of the virulence injectosome, with which they share considerable structural and amino acid sequence similarity [22-25]. The flagellar export machinery comprises an ATPase complex (FliHIJ) located in the cytoplasm, peripheral to the membrane. Immediately above the ATPase is a nonameric ring formed by the cytoplasmic domain of FlhA ($FlhA_C$), which functions as a subunit docking platform [20],[21],[26]. A recent cryo-ET map indicates that the FlhA family have a sea-horse-like structure, in which FlhAc forms the 'body' and the FlhA N-terminal region ($FlhA_N$) forms the 'head', which is fixed in the plane of the membrane [27]. $FlhA_N$ wraps around the base of a complex formed by FliPQR and the N-terminal sub-domain of FlhB ($FlhB_N$), and together

these form the FlhAB-FliPQR export gate that connects the cytoplasm to the central channel in the nascent flagellum, which is contiguous with the extracellular environment [22],[28]. $FlhB_N$ is connected *via* a linker ($FlhB_{CN}$) to the cytoplasmic domain of FlhB ($FlhB_C$), which is thought to sit between the $FlhA_N$ and $FlhA_C$ rings, where it functions as a docking site for early flagellar subunits [22],[14],[28].

The 'early' flagellar subunits that assemble to form the rod and hook substructures are not chaperoned: instead, the signals for targeting and export are found within the early subunits themselves. We have shown that one of these signals is a small hydrophobic sequence termed the gate recognition motif (GRM), which is essential for early subunit export [14]. This motif binds a surface exposed hydrophobic pocket on FlhBc [14]. Once subunits reach the export machinery, they must be unfolded before they can pass through the narrow channel formed by FliPQR-$FlhB_N$ into the central channel of the nascent flagellum, through which the subunits transit until they reach the tip and fold into the structure [22],[6]. Structural studies suggest that FliPQR-$FlhB_N$ adopts an energetically favourable closed conformation, possibly to maintain the membrane permeability barrier [22],[25],[29],[30]. This suggests that there must be a mechanism to trigger opening of the export gate when subunits dock at cytoplasmic face of the flagellar export machinery.

Here we sought to identify new export signals within flagellar rod/hook subunits, using the hook-cap subunit FlgD as a model export substrate. We show that the extreme N-terminus of rod/hook subunits contains a hydrophobic export signal and investigate its functional relationship to the subunit gate recognition motif (GRM).

73 **Results**

74 ***Identification of a hydrophobic export signal at the N-terminus of FlgD***

75 The N-terminal region of flagellar rod and hook subunits is required for their export
76 [12],[14]. Using the flagellar hook-cap protein FlgD as a model rod/hook subunit, we
77 sought to identify specific export signals within the N-terminus. A screen of ten FlgD
78 variants containing internal five-residue scanning deletions in the first 50 residues
79 (though FlgDΔ2-5 is a four-residue deletion, retaining the initial methionine) identified
80 just two variants defective for export into culture supernatant (**Fig. 1A**). Loss of
81 residues 2-5 caused a significant reduction in export, as did deletion of residues 36-
82 40, though to a lesser extent (**Fig. 1A**; [14]). We have shown that FlgD residues 36-
83 40 are the gate recognition motif (GRM) required for transient subunit docking at the
84 $FlhB_C$ component of the export gate [14]. The results suggest that the extreme N-
85 terminus might also be important for interaction with the export machinery.

86

87 To gain insight into the putative new signal, we screened for intragenic suppressor
88 mutations that could restore export of the FlgDΔ2-5 variant. A *Salmonella flgD* null
89 strain expressing *flgD*Δ2-5 *in trans* was inoculated into soft-tryptone agar and
90 incubated until 'spurs' of motile cell populations appeared. Sequencing of *flgD*Δ2-5
91 alleles from these motile populations identified ten different intragenic gain-of-
92 function mutations. These could be separated into two classes (**Fig. 1B**).

93

94 The first class of motile revertants carried *flgD*Δ2-5 alleles with missense mutations
95 that introduced small non-polar residues at the extreme N-terminus of FlgDΔ2-5 (**Fig.**
96 **1B**). Deletion of residues 2-5 (^{2}SIAV^{5}) had removed all small non-polar amino acids

97 from the first ten residue region of FlgD, effectively creating a new N-terminus
98 containing a combination of polar, charged or large non-polar residues (**Fig. S1**).
99 Analysis of other flagellar rod and hook subunit primary sequences revealed that in
100 every case their native N-terminal regions contain small non-polar residues
101 positioned upstream of the gate recognition motif (GRM residues 36-40; **Fig. S1**),
102 indicating that hydrophobicity may be key to the function of the N-terminal export
103 signal. Export assays performed with two representative motile revertant strains
104 carrying *flgDΔ2-5* variants with gain-of-function point mutations, those encoding
105 FlgDΔ2-5-N_8I and FlgDΔ2-5-T_{11}I, revealed that export of these subunits had
106 recovered to ~50% of the level observed for wild type FlgD (**Fig. 1C**; **Fig. S2; Fig.**
107 **S3**).
108
109 The second class of motile revertants carried *flgD*Δ2-5 alleles that had acquired
110 duplications or insertions introducing at least six additional residues between the
111 FlgDΔ2-5 N-terminus and the gate recognition motif (GRM; **Fig. 1B**). It seemed
112 possible that these insertions/duplications might have restored subunit export either
113 by insertion of amino acids that could function as a 'new' hydrophobic export signal,
114 or by restoring the position of an existing small hydrophobic residue or sequence
115 relative to the GRM.
116
117 To assess these possibilities, we tested whether export of FlgDΔ2-5 could be
118 recovered by inserting either polar (^{19}STSTST^{20}) or small non-polar (^{19}AGAGAG^{20})
119 residues in the FlgDΔ2-5 N-terminal region at a position equivalent to one of the
120 suppressing duplications (^{19}GSGSMT^{20}; **Fig. 1B and D**; **Fig. S3**). We reasoned that

121 if suppression by the additional sequence had been caused by repositioning an
122 existing small hydrophobic amino acid relative to the GRM, then any insertional
123 sequence (polar or non-polar) would restore export, while if suppression had resulted
124 from insertion of a 'new' export signal, then either the polar STSTST or non-polar
125 AGAGAG, but not both, could be expected to restore export.
126
127 We found that both the engineered FlgD variants (FlgDΔ2-5-^{19}AGAGAG^{20} and
128 FlgDΔ2-5-^{19}STSTST^{20}) were exported from a *Salmonella flgD* null strain as
129 effectively as the gain-of-function mutant FlgDΔ2-5-^{19}GSGSMT^{20} isolated from the
130 suppressor screen (**Fig. 1D**). This suggests that the insertions had repositioned a
131 sequence in the FlgDΔ2-5 N-terminus relative to the GRM to overcome the loss of
132 small hydrophobic residues.
133
134 ***The position of the hydrophobic export signal relative to the gate recognition***
135 ***motif is critical for rod and hook subunit export***
136 The discovery of intragenic suppressors of the FlgDΔ2-5 export defect indicated that
137 FlgD export requires a hydrophobic signal towards the subunit N-terminus and that
138 the position of this hydrophobic signal relative to the previously described GRM is
139 important. Sequence analysis of the gain-of-function FlgDΔ2-5 insertion variants
140 revealed that the insertions were all located between the GRM and valine$_{15}$ (V_{15}; **Fig.**
141 **1B**). We reasoned that the insertions repositioned valine$_{15}$ relative to the GRM, such
142 that it could perform the function of the N-terminal hydrophobic signal lost in FlgDΔ2-
143 5. To test this view, we replaced V_{15} with alanine in the gain-of-function variant
144 FlgDΔ2-5-^{19}(GSGSMT)^{20} and assayed its export in the *Salmonella flgD* null (**Fig. 2A**;

145 **Fig. S4**). Unlike the *flgD* null strain producing either the parental FlgDΔ2-5-
146 ^{19}(GSGSMT)^{20} or wild type FlgD, the *flgD* null carrying variant FlgDΔ2-5-
147 ^{19}(GSGSMT)^{20}-V_{15}A was non-motile, reflecting the variant's failure to export (**Fig.**
148 **2A**). This suggests that the V_{15} residue had indeed compensated for the missing N-
149 terminal hydrophobic signal.
150
151 By screening for intragenic suppressors of the motility defect associated with
152 FlgDΔ2-5-^{19}(GSGSMT)^{20}-V_{15}A, four gain-of-function missense mutations were
153 identified, M_7I, D_9A, T_{11}I and G_{14}V. All of these had introduced small hydrophobic
154 residues, all positioned at least 27 residues upstream of the GRM. These FlgDΔ2-5-
155 ^{19}(GSGSMT)^{20}-V_{15}A gain-of-function variants restored motility to the *Salmonella flgD*
156 null strain and were exported at levels similar to wildtype FlgD and FlgDΔ2-5-
157 ^{19}(GSGSMT)^{20} (**Fig. 2A**). These data confirm the importance of small non-polar
158 residues positioned upstream of the GRM.
159
160 Our results so far had indicated that the position of the FlgD N-terminal hydrophobic
161 export signal relative to the GRM was critical and suggested that, for export to occur
162 efficiently, at least 26 residues must separate the hydrophobic signal and the GRM
163 (**Fig 1C**). In the primary sequences of all *Salmonella* flagellar rod/hook subunits the
164 GRM is positioned ≥ 30 amino acids downstream of the subunit N-terminus (**Fig S1**),
165 suggesting that separation of the two signals by a minimum number of residues
166 might be a common feature among early flagellar subunits. To test this, a suite of
167 engineered *flgD* alleles was constructed that encoded FlgD variants in which
168 wildtype residues 9-32 were replaced with between one and four repeats of the six

169 amino acid sequence Gly-Ser-Thr-Asn-Ala-Ser (GSTNAS). Swimming motility and
170 export assays revealed that the minimum number of inserted GSTNAS repeats that
171 could support efficient FlgD export was three, equivalent to separation of the
172 hydrophobic N-terminal signal and the GRM by 24 residues (**Fig. 2B**; **Fig. S5**).
173 Below this threshold, FlgD export and swimming motility were strongly attenuated
174 (**Fig. 2B**). A further set of recombinant *flgD* alleles was constructed, which encoded
175 FlgDΔ9-32 variants carrying two GSTNAS repeats (hereafter termed $FlgD_{short}$)
176 directly followed by between one and five additional residues (**Fig. 2C**; **Fig. S5**).
177 Motility and FlgD export increased incrementally with the addition of each amino acid
178 (**Fig. 2C**). The data indicate that a low level of FlgD export is supported when the
179 hydrophobic N-terminal signal ($_{2}SIAV_{5}$) and the GRM ($_{36}FLTLL_{40}$) are separated by
180 19 residues, with export efficiency and swimming motility increasing as separation of
181 the export signals approaches the optimal 30 residues.
182
183 To further establish the requirement for a minimum number of residues between the
184 hydrophobic N-terminal signal and the GRM, we screened for intragenic suppressor
185 mutations that could restore swimming motility in a *flgD* null strain producing
186 $FlgD_{short}$. Sequencing of *flgD*$_{short}$ alleles from motile revertant strains identified 12
187 gain-of-function mutations that introduced additional residues between the
188 hydrophobic N-terminal signal and the GRM (**Fig. S6**). Swimming motility and FlgD
189 export was assessed for three *flgD* null strains expressing representative *flgD*$_{short}$
190 gain-of-function variants and all showed increased FlgD subunit export and
191 swimming motility compared to the *flgD* null expressing *flgD*$_{short}$ (**Fig. 2D**; **Fig. S6**).

192 The data confirm that the position of the hydrophobic N-terminal signal relative to the
193 GRM is critical for efficient FlgD subunit export.
194
195 To establish that this is a general requirement for the export of other rod and hook
196 subunits, engineered alleles of *flgE* (hook) and *flgG* (rod) were constructed that
197 encoded variants in which FlgE residues 9-32 or FlgG residues 11-35 were either
198 deleted ($FlgE_{short}$ and $FlgG_{short}$) or replaced with four repeats of the sequence
199 GSTNAS (**Fig. 3**; **Fig. S7**). As had been observed for $FlgD_{short}$, export of the
200 $FlgE_{short}$ and $FlgG_{short}$ variants was severely attenuated compared to wild type FlgE
201 and FlgG (**Fig. 3**). Furthermore, insertion of four GSTNAS repeats into $FlgE_{short}$ and
202 $FlgG_{short}$ recovered subunit export to wild type levels, indicating that the minimum
203 separation of the hydrophobic N-terminal signal and the GRM is a feature throughout
204 rod and hook subunits (**Fig. 3**).
205
206 ***Sequential engagement of the subunit GRM and hydrophobic N-terminal***
207 ***export signal by the flagellar export machinery***
208 Having identified a new hydrophobic N-terminal export signal and established that its
209 position relative to the GRM was critical, we next wanted to determine the order in
210 which the signals were recognised/engaged by the export machinery. The signals
211 might be recognised simultaneously, with both being required for initial entry of
212 rod/hook subunits into the export pathway. Alternatively, they might be recognised
213 sequentially. If this were the case, then a subunit variant that possessed the 'first'
214 signal but was deleted for the 'second' signal might enter the export pathway but fail
215 to progress, becoming stalled at a specific step to block the pathway and prevent

216 export of wild type subunits. To test if FlgDΔ2-5 or FlgDΔGRM stalled in the export
217 pathway, recombinant expression vectors encoding these variants or wild type FlgD
218 were introduced into a *Salmonella* Δ*recA* strain that is wild type for flagellar export
219 (**Fig. 4**). We could then assess whether the variant FlgD constructs could interfere *in*
220 *trans* with the wild type flagellar export. We saw that FlgDΔ2-5 inhibited motility and
221 export of the FliK and FlgK flagellar subunits, whereas FlgDΔGRM did not (**Fig. 4B**
222 **and C**). The data indicate that FlgDΔ2-5 enters the flagellar export pathway and
223 stalls at a critical point, blocking export. In contrast, FlgDΔGRM does not stall or
224 block export.
225
226 To determine whether FlgDΔ2-5 stalls at a point before or after subunit docking at
227 the $FlhB_C$ component of the flagellar export gate *via* the GRM, a recombinant vector
228 encoding a FlgD variant in which both export signals were deleted (FlgDΔ2-5ΔGRM)
229 was constructed. If loss of the hydrophobic N-terminal signal had caused subunits to
230 stall after docking at $FlhB_C$, then additional deletion of the subunit GRM would relieve
231 this block. Motility and subunit export assays revealed that the *Salmonella* Δ*recA*
232 strain producing FlgDΔ2-5ΔGRM displayed swimming motility and levels of FliK and
233 FlgK subunit export similar to cells producing FlgDΔGRM (**Fig. 4B and C**). The data
234 suggest that FlgDΔ2-5 stalls after docking at the $FlhB_C$ export gate, preventing
235 docking of other early subunits.
236
237 It seemed possible that subunit docking *via* the GRM to the $FlhB_C$ export gate might
238 position the hydrophobic N-terminal signal in close proximity to its recognition site on
239 the export machinery. If this were the case, 'short' subunit variants containing

240 deletions that decreased the number of residues between the hydrophobic N-
241 terminal signal and the GRM might also stall at $FlhB_C$, and this stalling might be
242 relieved by additional deletion of the GRM. To test this, recombinant expression
243 vectors encoding 'short' subunit variants ($FlgE_{short}$ or $FlgD_{short}$), 'short' subunit
244 variants additionally deleted for the GRM ($FlgE_{short}$ΔGRM or $FlgD_{short}$ΔGRM) or wild
245 type FlgE or FlgD were introduced into a *Salmonella* Δ*recA* strain (**Fig 5**). Compared
246 to the wild type subunits expressed *in trans*, the 'short' subunits inhibited swimming
247 motility and the export of other flagellar subunits (FliD, FliK, FlgK), whereas
248 $FlgE_{short}$ΔGRM and $FlgD_{short}$ΔGRM did not (**Fig 5**). Taken together with the data
249 presented in Figure 4, the results indicate that the subunit GRM and the hydrophobic
250 N-terminal signal are recognised sequentially, with subunits first docking at $FlhB_C$ *via*
251 the GRM, which positions the hydrophobic N-terminal signal for subsequent
252 interactions with the export machinery (**Fig 4D**).
253

254 **Mutations that promote opening of the export gate partially compensate for**
255 **incorrect positioning of the subunit N-terminal export signal**

256 The accruing data indicated that subunit docking at $FlhB_C$ might correctly position the
257 hydrophobic N-terminal signal for recognition by the export machinery. To model the
258 position of $FlhB_C$ relative to other components of the export machinery, we placed
259 the structures of $FlhB_C$ and the FliPQR-$FlhB_N$ export gate into the tomographic
260 reconstruction of the *Salmonella* SPI-1 type III secretion system (**Fig 6B**; [31]). The
261 model indicated that FliPQR-$FlhB_N$ and the subunit docking site on $FlhB_C$ are
262 separated by a minimum distance of ~78 Å, and that $FlhB_C$ is positioned no more
263 than ~22-45 Å from FlhA (Fig 6A; [27]). Taking FlgD as a model early flagellar

264 subunit, the distance between the FlgD N-terminal hydrophobic signal and the GRM
265 was found to be in the range of ~45 Å (α-helix) to ~105 Å (unfolded contour length),
266 depending on the predicted structure adopted by the subunit N-terminus (Fig 6A).
267 Based on these estimates, it seemed feasible that the hydrophobic N-terminal signal
268 of a subunit docked at $FlhB_C$ could contact either FlhA or the FliPQR-$FlhB_N$ complex,
269 and that this interaction might trigger opening of the export gate [27],[30],[22]. If this
270 were true, mutations that promote the open conformation of the export gate might
271 compensate for the incorrect positioning of the hydrophobic N-terminal export signal
272 in 'short' rod/hook subunits. One such export gate mutation, FliP-M_{210}A, has been
273 shown to increase ion conductance across the bacterial inner membrane, indicating
274 that this gate variant fails to close efficiently [29].
275
276 To test whether the FliP-M_{210}A variant gate could promote export of 'short' subunits,
277 in which the distance between the hydrophobic N-terminal signal and the GRM was
278 reduced, a recombinant expression vector encoding $FlgD_{short}$ was introduced into
279 *Salmonella flgD* null strains in which the *fliP* gene had been replaced with
280 recombinant genes encoding either a functional FliP variant with an internal HA-tag
281 (designated wild type gate) or the equivalent HA-tagged FliP-M_{210}A variant
282 (designated M_{210}A gate; **Fig. 6C**; **Fig. S8**). The swimming motility of these strains
283 was found to be consistently stronger in the strain producing the M_{210}A gate
284 compared to the strain with the wild type gate, with the motility halo of the *fliP*-
285 M210A-Δ*flgD* strain expressing $FlgD_{short}$ having a 50% greater diameter than that of
286 the wild type *fliP*-Δ*flgD* strain expressing $FlgD_{short}$ (**Fig. 6D**). This increase in motility
287 indicated that the defect caused by incorrect positioning of the hydrophobic N-

288 terminal signal relative to the GRM in $FlgD_{short}$ could indeed be partially
289 compensated by promoting the gate open conformation.
290
291 **Discussion**
292 T3SS substrates contain N-terminal export signals, though these signals have not
293 been fully defined and how they promote subunit export remains unclear. Here, we
294 characterised a new hydrophobic N-terminal export signal in early flagellar rod/hook
295 subunits and showed that the position of this signal relative to the known subunit
296 gate recognition motif (GRM) is key to export.
297
298 Loss of the hydrophobic N-terminal signal in the hook cap subunit FlgD had a
299 stronger negative effect on subunit export than deletion of the GRM that enables
300 subunit docking at $FlhB_C$, suggesting that the hydrophobic N-terminal signal may be
301 required to trigger an essential export step. A suppressor screen showed that the
302 export defect caused by deleting the hydrophobic N-terminal signal could be
303 overcome by mutations that either reintroduced small non-polar amino acids
304 positioned 3-7 residues from the subunit N-terminus (*e.g.* M_7I), or introduced
305 additional residues between V_{15} and the GRM. In such 'gain of function' strains
306 containing insertions, changing V_{15} to alanine abolished subunit export, which was
307 rescued by re-introduction of small non-polar residues close to the N-terminus.
308 These data point to an essential export function for small non-polar residues close to
309 the N-terminus of rod/hook subunits.
310

311 It was fortuitous that we chose FlgD as the model for early flagellar subunit. All early
312 subunits contain small hydrophobic residues close to the N-terminus, but FlgD is
313 unique in that only four (I_3, A_4, V_5 and V_{15}) of its first 25 residues are small and non-
314 polar (**Fig. S1**). Indeed, there are only three other small hydrophobic residues
315 between the FlgD N-terminus and the GRM (**Fig. 1**). While deletion of residues 2-5 in
316 FlgD removes the critical hydrophobic N-terminal signal, similar deletions in the N-
317 terminal regions of other rod/hook subunits reposition existing small non-polar
318 residues close to the N-terminus (**Fig. S1**). This is perhaps why previous deletion
319 studies in early flagellar subunits have failed to identify the hydrophobic N-terminal
320 signal [14],[37],[38].
321
322 The finding that subunits lacking the hydrophobic N-terminal export signal, but not
323 the GRM, stalled during export suggested that these two signals were recognised by
324 the flagellar export machinery in a specific order. Mutant variants of other flagellar
325 export substrates or export components have been observed to block the export
326 pathway. For example, a FlgN chaperone variant lacking the C-terminal 20 residues
327 stalls at the FliI ATPase [39], while a GST-tagged FliJ binds FlhA but is unable to
328 associate correctly with FliI so blocking wild type FliJ interaction with FlhA [40].
329 These attenuations can be reversed by further mutations that disrupt the stalling
330 interactions. This was also observed for FlgDΔ2-5. Loss of the hydrophobic N-
331 terminal signal resulted in a dominant-negative effect on motility and flagellar export,
332 but this was abolished by subsequent deletion of the GRM. This indicates that
333 FlgDΔ2-5 stalls in the export pathway at $FlhB_C$, blocking the binding site for early
334 flagellar subunits. These data are consistent with sequential recognition of the two

335 export signals: the GRM first docking subunits at $FlhB_C$, and positioning the
336 hydrophobic N-terminal signal to trigger the next export step.
337
338 The position of the subunit hydrophobic N-terminal export signal relative to the GRM
339 appears critical for export. Engineering of *flgD* to encode variants in which the region
340 between the N-terminus and the GRM was replaced with polypeptide sequences of
341 varying lengths showed that these signals must be separated by a minimum of 19
342 residues for detectable export, with substantial export requiring separation by 30
343 residues (**Fig. 3**). When subunits dock at $FlhB_C$, which is likely situated within or just
344 below the plane of the inner membrane, the hydrophobic N-terminal signal is
345 positioned close to the FlhAB-FliPQR export gate (**Fig. 6B**). Subunits in which the
346 GRM and N-terminal signal are brought closer together stall at $FlhB_C$, suggesting
347 that the hydrophobic N-terminal signal is unable to contact its recognition site on the
348 export machinery (**Figs. 5, 6A and 6B**). In all flagellar rod/hook subunits, the GRM is
349 positioned at least 30 residues from the N-terminus (**Fig. S1**). The physical distance
350 between the two signals will depend on the structure adopted by the subunit N-
351 terminus (**Fig. 6A**). The N-terminal region of flagellar subunits is often unstructured
352 in solution [11-15],[32], and such disorder may be an intrinsic feature of flagellar
353 export signals [11-15],[33],[34], as is typical in other bacterial N-terminal export
354 signals such as those in substrates of the Sec and Tat systems [35],[36].
355 Unstructured signals may facilitate multiple interactions with different binding
356 partners during export, and in the case of export systems that transport unfolded
357 proteins they may aid initial entry of substrates into narrow export channels [35].
358

359 As yet, nothing is known about the structure of the subunit N-terminal domain upon
360 interaction with the flagellar export machinery. Signal peptides in TAT pathway
361 substrates switch between disordered and α-helical conformations depending on the
362 hydrophobicity of the environment [41]. It therefore seems likely that local
363 environments along the flagellar export pathway will influence the conformation of
364 subunit export signals [42],[22]. In flagellar subunits, if the region between the
365 hydrophobic N-terminal signal and the GRM is unstructured and extended, this
366 would correspond to a polypeptide contour length of approximately 72-105 Å (where
367 the length of one amino acid is ~3.6 Å). If the same region were to fold as an α-helix,
368 its length would be approximately 30-36 Å (where one amino acid rises every ~1.5
369 Å). Without further structural information on subunit interactions with the flagellar
370 export machinery and the precise position of FlhBC within the machinery, it is difficult
371 to determine precisely where the hydrophobic N-terminal signal contacts the
372 machinery.
373
374 We speculate that one function of the subunit hydrophobic N-terminal signal might
375 be to trigger opening of the FlhAB-FliPQR export gate, which rests in an
376 energetically favourable closed conformation to maintain the permeability barrier
377 across the bacterial inner membrane [29],[22],[30],[27]. The atomic resolution
378 structure of FliPQR showed that it contains three gating regions [22]. FliR provides a
379 loop (the R-plug) that sits within the core of the structure. Below this, five copies of
380 FliP each provides three methionine residues that together form a methionine-rich
381 ring under which ionic interactions between FliQ residues hold the base of the
382 structure shut (Q-latch).

383 A recent structure of a substrate trapped within the vT3SS revealed conformational
384 changes within the export gate [43]. These changes include a rearrangement of the
385 M-gate methione residues and folding up of the FliR plug to allow substrate passage.
386 If the function of the subunit hydrophobic N-terminal signal was to trigger opening of
387 this gate, we hypothesised that mutations which destabilised the gate's closed
388 conformation would suppress the motility defect associated with $FlgD_{short}$, in which
389 the distance between the N-terminal signal and the GRM is reduced. Introduction of
390 the FliP-M_{210}A mutation, which partially destabilises the gate's closed state, did
391 indeed partly suppress the $FlgD_{short}$ motility defect. We did not find export gate
392 variants that completely destabilised gate closure, but it may be that such mutations
393 disrupt the membrane permeability barrier [29]. This could also explain why in
394 screens for suppressors of FlgDΔ2-5 or $FlgD_{short}$ we did not isolate mutations in
395 genes encoding export gate components (data not shown).
396
397 The surface-exposed hydrophobic GRM-binding pocket on $FlhB_C$ is well conserved
398 across the T3SS SctU family, to which FlhB belongs [14],[44],[45]. Furthermore, the
399 GRM is conserved in all four injectosome early subunits (SctI, SctF, SctP, OrgC) and
400 is located at least 30 residues away from small hydrophobic residues near the
401 subunit N-terminus. It therefore seems plausible that the 'dual signal' mechanism we
402 propose for early flagellar export operates in all T3SS pathways.
403
404 Based on the genetic and biochemical work presented here, we propose a model of
405 sequential recognition of export signals at the T3SS export machinery. Early
406 substrates engage with the GRM-binding pocket on $FlhB_C$, positioning the subunit N-

407 terminal hydrophobic signal to contact its recognition site. Given that $FlhB_C$ is
408 positioned directly below the FliPQR-$FlhB_N$ gate, the N-terminal hydrophobic signal
409 of substrates docked at $FlhB_C$ would be suitably positioned to trigger export gate
410 opening. Based on the location of $FlhB_C$ and the relative position between export
411 signals, the N-terminal hydrophobic signal could trigger gate opening by indirect
412 interactions with FlhA/FlhB or *via* direct interactions with the FliPQR-$FlhB_N$ export
413 gate components.
414
415 In many other pathways, the presence of a substrate triggers opening or assembly of
416 the export channel. The outer membrane chitin transporter in *Vibrio* adopts a closed
417 conformation in which the N-terminus of a neighbouring subunit acts as a pore plug
418 [46]. Chitin binding to the transporter ejects the plug, opening the transport channel
419 and allowing chitin transport [45]. In the Sec pathway, interactions of SecA,
420 ribosomes or pre-proteins with SecYEG can induce conformational changes that
421 promote channel opening [47-49],[35]. In the TAT system, which transports folded
422 substrates across the cytoplasmic membrane, substrate binding to the TatBC
423 complex triggers association with, and subsequent polymerisation of, TatA, which is
424 required for substrate translocation [50],[36]. All of these mechanisms serve both to
425 conserve energy and prevent disruption of the membrane permeability barrier. Our
426 data suggest that in a comparable way the signal of non-polar residues within the N-
427 termini of early rod/hook subunits trigger export gate opening.

428 **Methods**

429 **Bacterial strains, plasmids and growth conditions**

430 *Salmonella* strains and plasmids used in this study are listed in **Supplementary**
431 **Table 1**. The Δ*flgD*::K_m^R strain in which the *flgD* gene was replaced by a kanamycin
432 resistance cassette was constructed using the λ Red recombinase system [58].
433 Strains containing chromosomally encoded FliP variants were constructed by aph-I-
434 SceI Kanamycin resistance cassette replacement using pWRG730 [59].
435 Recombinant proteins were expressed in *Salmonella* from the isopropyl β-D-
436 thiogalactoside-inducible (IPTG) inducible plasmid pTrc99a [60]. Bacteria were
437 cultured at 30–37 °C in Luria-Bertani (LB) broth containing ampicillin (100 µg/ml).
438

439 **Flagellar subunit export assay**

440 *Salmonella* strains were cultured at 37 °C in LB broth containing ampicillin and IPTG
441 to mid-log phase (OD_{600nm} 0.6-0.8). Cells were centrifuged (6000*g*, 3 min) and
442 resuspended in fresh media and grown for a further 60 min at 37 °C. The cells were
443 pelleted by centrifugation (16,000*g*, 5 min) and the supernatant passed through a 0.2
444 µm nitrocellulose filter. Proteins were precipitated with 10% trichloroacetic acid
445 (TCA) and 1% Triton-X100 on ice for 1 hour, pelleted by centrifugation (16,000*g*, 10
446 min), washed with ice-cold acetone and resuspended in SDS-PAGE loading buffer
447 (volumes calibrated according to cell densities). Fractions were analysed by
448 immunoblotting.
449
450
451

452 **Motility assays**

453 For swimming motility, cultures were grown in LB broth to A600nm 1. Two microliters
454 of culture were inoculated into soft tryptone agar (0.3% agar, 10 g/L tryptone, 5g/L
455 NaCl) containing ampicillin (100 µg/ml). Plates were incubated at 37 °C for between
456 4 and 6 hours unless otherwise stated.

457

458 **Isolation of motile strains carrying suppressor mutations**

459 Cells of the *Salmonella flgD* null strain transformed with plasmids expressing FlgD
460 variants (FlgDΔ2-5, FlgDΔ2-5-^{19}GSGSMT^{20}-V15A or FlgD$_{short}$) were cultured at 37
461 °C in LB broth containing ampicillin (100 µg/ml) to mid-log phase and inoculated into
462 soft tryptone agar (0.3% agar, 10 g/L tryptone, 5g/L NaCl) containing ampicillin (100
463 µg/ml). Plates were incubated at 30 °C until motile 'spurs' appeared. Cells from the
464 spurs were streaked to single colony and cultured to isolate the *flgD* encoding
465 plasmid. Plasmids were transformed into the *Salmonella flgD* null strain to assess
466 whether the plasmids were responsible for the motile suppressor phenotypes.
467 Plasmids were sequenced to identify the suppressor mutations.

468

469 **Quantification and statistical analysis**

470 Experiments were performed at least three times. Immunoblots were quantified using
471 Image Studio Lite. The unpaired two-tailed Student's *t*-test was used to determine *p*-
472 values and significance was determined as $*p < 0.05$. Data are represented as mean
473 ± standard error of the mean (SEM), unless otherwise specified and reported as
474 biological replicates.

475

Author contributions

Owain J. Bryant: Conceptualization, Data curation, Investigation, Formal analysis, Methodology, Visualisation, Writing – original draft, Writing – review & editing. **Paraminder Dhillon**: Conceptualization, Data curation, Investigation, Formal analysis, Methodology, Visualisation, Writing – review & editing. **Colin Hughes**: Conceptualization, Data curation, Formal analysis, Funding acquisition, Investigation, Methodology, Project administration, Resources, Supervision, Visualisation, Writing – review & editing. **Gillian M. Fraser**: Conceptualization, Data curation, Formal analysis, Funding acquisition, Investigation, Methodology, Project administration, Resources, Supervision, Visualisation, Writing – original draft, Writing – review & editing.

Competing interests

The authors declare no competing interests.

Acknowledgements

This work was funded by grants from the Biotechnology and Biological Sciences Research Council (BB/M007197/1) to G.M.F, the Wellcome Trust (082895/Z/07/Z) to C.H. and G.M.F., a Biotechnology and Biological Sciences Research Council studentship to P.D., and a University of Cambridge John Lucas Walker studentship to O.J.B.

Materials & Correspondence

Materials are available from the corresponding author upon request.

500 **References**

501 [1] L. D. B. Evans, C. Hughes, and G. M. Fraser, “Building a flagellum in biological
502 outer space.,” *Microb. cell (Graz, Austria)*, 2014.

503 [2] W. Deng *et al.*, “Assembly, structure, function and regulation of type III
504 secretion systems,” *Nature Reviews Microbiology*. 2017.

505 [3] D. Büttner and S. Y. He, “Type III protein secretion in plant pathogenic
506 bacteria,” *Plant Physiol.*, 2009.

507 [4] M. E. Konkel *et al.*, “Secretion of virulence proteins from Campylobacter jejuni
508 is dependent on a functional flagellar export apparatus,” *J. Bacteriol.*, 2004.

509 [5] M. Dongre *et al.*, “Flagella-mediated secretion of a novel Vibrio cholerae
510 cytotoxin affecting both vertebrate and invertebrate hosts,” *Commun. Biol.*,
511 2018.

512 [6] L. D. B. Evans, C. Hughes, and G. M. Fraser, “Building a flagellum outside the
513 bacterial cell,” *Trends in Microbiology*. 2014.

514 [7] T. Minamino and K. Namba, “Distinct roles of the FliI ATPase and proton
515 motive force in bacterial flagellar protein export,” *Nature*, vol. 451, no. 7177,
516 pp. 485–488, 2008.

517 [8] K. Paul, M. Erhardt, T. Hirano, D. F. Blair, and K. T. Hughes, “Energy source of
518 flagellar type III secretion,” *Nature*, 2008.

519 [9] A. W. Williams, S. Yamaguchi, F. Togashi, S. I. Aizawa, I. Kawagishi, and R.
520 M. Macnab, “Mutations in fliK and flhB affecting flagellar hook and filament
521 assembly in Salmonella typhimurium,” *J. Bacteriol.*, 1996.

522 [10] G. M. Fraser, T. Hirano, H. U. Ferris, L. L. Devgan, M. Kihara, and R. M.
523 Macnab, “Substrate specificity of type III flagellar protein export in Salmonella

524 is controlled by subdomain interactions in FlhB.," *Mol. Microbiol.*, 2003.
525 [11] G. Kuwajima, I. Kawagishi, M. Homma, J. Asaka, E. Kondo, and R. M.
526 Macnab, "Export of an N-terminal fragment of Escherichia coli flagellin by a
527 flagellum-specific pathway.," *Proc. Natl. Acad. Sci.*, 2006.
528 [12] T. Minamino and R. M. Macnab, "Components of the Salmonella flagellar
529 export apparatus and classification of export substrates," *J. Bacteriol.*, 1999.
530 [13] M. G. Kornacker and A. Newton, "Information essential for cell-cycle-
531 dependent secretion of the 591-residue Caulobacter hook protein is confined
532 to a 21-amino-acid sequence near the N-terminus," *Mol. Microbiol.*, 1994.
533 [14] L. D. B. Evans, S. Poulter, E. M. Terentjev, C. Hughes, and G. M. Fraser, "A
534 chain mechanism for flagellum growth," *Nature*, vol. 504, no. 7479, pp. 287–
535 290, 2013.
536 [15] B. M. Végh, P. Gál, J. Dobó, P. Závodszky, and F. Vonderviszt, "Localization
537 of the flagellum-specific secretion signal in Salmonella flagellin," *Biochem.*
538 *Biophys. Res. Commun.*, 2006.
539 [16] P. Wattiau, B. Bernier, P. Deslée, T. Michiels, and G. R. Cornelis, "Individual
540 chaperones required for Yop secretion by Yersinia," *Proc. Natl. Acad. Sci. U.*
541 *S. A.*, 1994.
542 [17] G. M. Fraser, J. C. Q. Bennett, and C. Hughes, "Substrate-specific binding of
543 hook-associated proteins by FlgN and FliT, putative chaperones for flagellum
544 assembly," *Mol. Microbiol.*, vol. 32, no. 3, pp. 569–580, 1999.
545 [18] J. Thomas, G. P. Stafford, and C. Hughes, "Docking of cytosolic chaperone-
546 substrate complexes at the membrane ATPase during flagellar type III protein
547 export.," *Proc. Natl. Acad. Sci. U. S. A.*, vol. 101, no. 11, pp. 3945–3950, 2004.

548 [19] Y. Akeda and J. E. Galán, “Chaperone release and unfolding of substrates in
549 type III secretion,” *Nature*, 2005.
550 [20] G. Bange, N. Kümmerer, C. Engel, G. Bozkurt, K. Wild, and I. Sinning, “FlhA
551 provides the adaptor for coordinated delivery of late flagella building blocks to
552 the type III secretion system.,” *Proc. Natl. Acad. Sci. U. S. A.*, vol. 107, no. 25,
553 pp. 11295–11300, 2010.
554 [21] M. Kinoshita, N. Hara, K. Imada, K. Namba, and T. Minamino, “Interactions of
555 bacterial flagellar chaperone-substrate complexes with FlhA contribute to co-
556 ordinating assembly of the flagellar filament,” *Mol. Microbiol.*, vol. 90, no. 6, pp.
557 1249–1261, 2013.
558 [22] L. Kuhlen *et al.*, “Structure of the core of the type iii secretion system export
559 apparatus,” *Nat. Struct. Mol. Biol.*, 2018.
560 [23] P. Abrusci *et al.*, “Architecture of the major component of the type III secretion
561 system export apparatus,” *Nat. Struct. Mol. Biol.*, vol. 20, no. 1, pp. 99–104,
562 2012.
563 [24] K. Eichelberg, C. C. Ginocchio, and J. E. Galan, “Molecular and functional
564 characterization of the Salmonella typhimurium invasion genes invB and invC:
565 Homology of InvC to the F0F1 ATPase family of proteins,” *J. Bacteriol.*, 1994.
566 [25] S. Johnson, L. Kuhlen, J. C. Deme, P. Abrusci, and S. M. Lea, “The Structure
567 of an Injectisome Export Gate Demonstrates Conservation of Architecture in
568 the Core Export Gate between Flagellar and Virulence Type III Secretion
569 Systems,” *MBio*, 2019.
570 [26] Q. Xing, K. Shi, A. Portaliou, P. Rossi, A. Economou, and C. G. Kalodimos,
571 “Structures of chaperone-substrate complexes docked onto the export gate in

572 a type III secretion system," *Nat. Commun.*, 2018.
573 [27] C. Butan, M. Lara-Tejero, W. Li, J. Liu, and J. E. Galán, "High-resolution view
574 of the type III secretion export apparatus in situ reveals membrane remodeling
575 and a secretion pathway.," *Proc. Natl. Acad. Sci. U. S. A.*, 2019.
576 [28] S. Mizuno, H. Amida, N. Kobayashi, S. I. Aizawa, and S. I. Tate, "The NMR
577 structure of FliK, the trigger for the switch of substrate specificity in the flagellar
578 type III secretion apparatus," *J. Mol. Biol.*, 2011.
579 [29] E. Ward, T. T. Renault, E. A. Kim, M. Erhardt, K. T. Hughes, and D. F. Blair,
580 "Type-III secretion pore formed by flagellar protein FliP," *Mol. Microbiol.*, 2018.
581 [30] L. Kuhlen *et al.*, "The substrate specificity switch FlhB assembles onto the
582 export gate to regulate type three secretion," *Nat. Commun.*, 2020.
583 [31] V. A. Meshcheryakov, A. Kitao, H. Matsunami, and F. A. Samatey, "Inhibition
584 of a type III secretion system by the deletion of a short loop in one of its
585 membrane proteins," *Acta Crystallogr. Sect. D Biol. Crystallogr.*, 2013.
586 [32] F. Vonderviszt, R. Ishima, K. Akasaka, and S. I. Aizawa, "Terminal disorder: A
587 common structural feature of the axial proteins of bacterial flagellum?," *J. Mol.*
588 *Biol.*, 1992.
589 [33] C. Weber-Sparenberg *et al.*, "Characterization of the type III export signal of
590 the flagellar hook scaffolding protein FlgD of Escherichia coli," *Arch. Microbiol.*,
591 2006.
592 [34] S. I. Aizawa, F. Vonderviszt, R. Ishima, and K. Akasaka, "Termini of
593 Salmonella flagellin are disordered and become organized upon
594 polymerization into flagellar filament," *J. Mol. Biol.*, 1990.
595 [35] A. Tsirigotaki, J. De Geyter, N. Šoštarić, A. Economou, and S. Karamanou,

596 “Protein export through the bacterial Sec pathway,” *Nature Reviews*
597 *Microbiology*. 2017.
598 [36] T. Palmer and B. C. Berks, “The twin-arginine translocation (Tat) protein export
599 pathway,” *Nature Reviews Microbiology*. 2012.
600 [37] T. Hirano, S. Shibata, K. Ohnishi, T. Tani, and S. I. Aizawa, “N-terminal signal
601 region of FliK is dispensable for length control of the flagellar hook,” *Mol.*
602 *Microbiol.*, 2005.
603 [38] T. Minamino, B. González-Pedrajo, K. Yamaguchi, S. I. Aizawa, and R. M.
604 Macnab, “FliK, the protein responsible for flagellar hook length control in
605 Salmonella, is exported during hook assembly,” *Mol. Microbiol.*, 1999.
606 [39] J. Thomas, G. P. Stafford, and C. Hughes, “Docking of cytosolic chaperone-
607 substrate complexes at the membrane ATPase during flagellar type III protein
608 export,” *Proc. Natl. Acad. Sci.*, 2004.
609 [40] T. Ibuki, Y. Uchida, Y. Hironaka, K. Namba, K. Imada, and T. Minamino,
610 “Interaction between FliJ and FlhA, components of the bacterial flagellar type iii
611 export apparatus,” *J. Bacteriol.*, 2013.
612 [41] M. San Miguel, R. Marrington, P. M. Rodger, A. Rodger, and C. Robinson, “An
613 Escherichia coli twin-arginine signal peptide switches between helical and
614 unstructured conformations depending on the hydrophobicity of the
615 environment,” *Eur. J. Biochem.*, 2003.
616 [42] M. Erhardt *et al.*, “Mechanism of type-III protein secretion: Regulation of FlhA
617 conformation by a functionally critical charged-residue cluster,” *Mol. Microbiol.*,
618 vol. 104, no. 2, pp. 234–249, 2017.
619 [43] S. Miletic, D. Fahrenkamp, N. Goessweiner-Mohr, J. Wald, M. Pantel, O.

620 Vesper, V. Kotov, and T. Marlovits. "Substrate-engaged type III secretion
621 system structures reveal gating mechanism for unfolded protein translocation"
622 bioRxiv., **doi:** https://doi.org/10.1101/2020.12.17.423328
623 [44] R. Zarivach *et al.*, “Structural analysis of the essential self-cleaving type III
624 secretion proteins EscU and SpaS,” *Nature*, 2008.
625 [45] G. T. Lountos, B. P. Austin, S. Nallamsetty, and D. S. Waugh, “Atomic
626 resolution structure of the cytoplasmic domain of Yersinia pestis YscU, a
627 regulatory switch involved in type III secretion,” *Protein Sci.*, 2009.
628 [46] A. Aunkham *et al.*, “Structural basis for chitin acquisition by marine Vibrio
629 species,” *Nat. Commun.*, 2018.
630 [47] Y. Ge, A. Draycheva, T. Bornemann, M. V. Rodnina, and W. Wintermeyer,
631 “Lateral opening of the bacterial translocon on ribosome binding and signal
632 peptide insertion,” *Nat. Commun.*, 2014.
633 [48] J. Zimmer, Y. Nam, and T. A. Rapoport, “Structure of a complex of the ATPase
634 SecA and the protein-translocation channel,” *Nature*, 2008.
635 [49] R. M. Voorhees, I. S. Fernández, S. H. W. Scheres, and R. S. Hegde,
636 “Structure of the mammalian ribosome-Sec61 complex to 3.4 Å resolution,”
637 *Cell*, 2014.
638 [50] H. Mori and K. Cline, “A twin arginine signal peptide and the pH gradient
639 trigger reversible assembly of the thylakoid ΔpH/Tat translocase,” *J. Cell Biol.*,
640 2002.
641 [51] L. D. B. Evans, P. M. Bergen, O. J. Bryant, and G. M. Fraser, “Interactions of
642 flagellar structural subunits with the membrane export machinery,” in *Methods
643 in Molecular Biology*, 2017.

644 [53] F. H. Login and H. Wolf-Watz, “YscU/FlhB of Yersinia pseudotuberculosis
645 harbors a C-terminal type III secretion signal,” *J. Biol. Chem.*, 2015.
646 [54] S. Frost, O. Ho, F. H. Login, C. F. Weise, H. Wolf-Watz, and M. Wolf-Watz,
647 “Autoproteolysis and Intramolecular Dissociation of Yersinia YscU Precedes
648 Secretion of Its C-Terminal Polypeptide YscUCC,” *PLoS One*, 2012.
649 [55] T. Minamino, Y. V. Morimoto, N. Hara, and K. Namba, “An energy transduction
650 mechanism used in bacterial flagellar type III protein export,” *Nat. Commun.*,
651 2011.
652 [56] M. Baba *et al.*, “Rotation of artificial rotor axles in rotary molecular motors,”
653 *Proc. Natl. Acad. Sci.*, 2016.
654 [57] N. Hara, K. Namba, and T. Minamino, “Genetic characterization of conserved
655 charged residues in the bacterial flagellar type III export protein FlhA,” *PLoS*
656 *One*, vol. 6, no. 7, 2011.
657 [58] K. A. Datsenko and B. L. Wanner, “One-step inactivation of chromosomal
658 genes in Escherichia coli K-12 using PCR products,” *Proc. Natl. Acad. Sci. U.*
659 *S. A.*, 2000.
660 [59] S. Hoffmann, C. Schmidt, S. Walter, J. K. Bender, and R. G. Gerlach,
661 “Scarless deletion of up to seven methylaccepting chemotaxis genes with an
662 optimized method highlights key function of CheM in Salmonella
663 Typhimurium,” *PLoS One*, 2017.
664 [60] E. Amann, B. Ochs, and K. J. Abel, “Tightly regulated tac promoter vectors
665 useful for the expression of unfused and fused proteins in Escherichia coli,”
666 *Gene*, 1988.
667 [61] B. Hu, M. Lara-Tejero, Q. Kong, J. E. Galán, and J. Liu, “In Situ Molecular

668 Architecture of the Salmonella Type III Secretion Machine," *Cell*, 2017.
669 [62] T. Minamino and R. M. Macnab, "Domain structure of Salmonella FlhB, a
670 flagellar export component responsible for substrate specificity switching," *J.*
671 *Bacteriol.*, 2000.
672 [63] J. Kyte and R. F Doolittle, "A simple method for displaying the hydropathic
673 character of a protein". *J. Mol. Biol.*, 1982.
674
675
676

677 **Figure legends**

678 **Figure 1. Screening for export-defective FlgD variants**

679 **a.** Whole cell (cell) and supernatant (sec) proteins from late exponential phase
680 cultures of a *Salmonella flgD* null strain expressing wild type FlgD (FlgD) or its
681 variants (Δ2-5, Δ6-10, Δ11-15, Δ16-20, Δ21-25, Δ26-30, Δ31-35, Δ36-40, Δ41-45 or
682 Δ46-50) were separated by SDS (15%)-PAGE and analysed by immunoblotting with
683 anti-FlgD polyclonal antisera.

684 **b.** A schematic displaying the intragenic suppressor mutations within amino acids 1-
685 40 of FlgD isolated from the FlgDΔ2-5 variant. Small non-polar residues are
686 highlighted in orange. All suppressor mutations were located between the gate-
687 recognition motif (GRM, blue) and the extreme N-terminus, and can be separated
688 into two classes: insertions or duplications that introduced additional sequence
689 between valine-15 and the gate-recognition motif, or missense mutations that re-
690 introduce small non-polar residues at the N-terminus.

691 **c**. Whole cell (cell) and supernatant (sec) proteins from late exponential-phase
692 cultures of *Salmonella flgD* null strains expressing suppressor mutants isolated from
693 the FlgDΔ2-5 variant (FlgDΔ2-5-N_8I or FlgDΔ2-5-T_{11}I), FlgDΔ2-5 variant (-) or wild
694 type FlgD (FlgD) were separated by SDS (15%)-PAGE and analysed by
695 immunoblotting with anti-FlgD polyclonal antisera.

696 **d.** Whole cell (cell) and supernatant (sec) proteins from late exponential phase
697 cultures of *Salmonella flgD* null strains expressing wild type FlgD (FlgD), FlgDΔ2-5
698 (DΔ2-5) or variants of FlgDΔ2-5 containing between residues 19 and 20 a six-
699 residue insertion of either small non-polar (AGAGAG) residues (3x(AG)), polar

700 (STSTST) residues (3x(ST)), or the sequence from an isolated insertion suppressor
701 mutant (GSGSMT), were separated by SDS (15%)-PAGE and analysed by
702 immunoblotting with anti-FlgD polyclonal antisera.

703

704 **Figure 2. Export of FlgD variants in which the position of the N-terminal**
705 **hydrophobic export signal is varied relative to the gate recognition motif**
706 **(GRM)**

707 Whole cell (cell) and supernatant (sec) proteins from late exponential-phase cultures
708 of a *Salmonella flgD* null strain expressing suppressor mutants isolated from the
709 FlgDΔ2-5-^{19}(GSGSMT)^{20}-$V_{15}A$ variant ($V_{15}A$-M_7I, $V_{15}A$-D_9A, $V_{15}A$-$T_{11}I$, $V_{15}A$-$G_{14}V$),
710 their parent FlgD variant FlgDΔ2-5-^{19}(GSGSMT)^{20}-$V_{15}A$ (labelled as $V_{15}A$), FlgDΔ2-
711 5-^{19}(GSGSMT)^{20} (labelled as -) or wild type FlgD (FlgD) were separated by SDS
712 (15%)-PAGE and analysed by immunoblotting with anti-FlgD polyclonal antisera.
713 Swimming motility (bottom panel; 0.25% soft tryptone agar) of the same strains was
714 assayed at 37ºC for 4-6 hours.

715 **b**. Whole cell (cell) and supernatant (sec) proteins from late exponential-phase
716 cultures of a *Salmonella flgD* null strain expressing wild type FlgD (FlgD), FlgDΔ9-32
717 or its variants in which residues 9-32 were replaced by between one and four six-
718 residue repeats of Gly-Ser-Thr-Asn-Ala-Ser (Δ9-32 4xRpt, Δ9-32 3xRpt, Δ9-32
719 2xRpt or Δ9-32 1xRpt) were separated by SDS (15%)-PAGE and analysed by
720 immunoblotting with anti-FlgD polyclonal antisera. Swimming motility (bottom panel;
721 0.25% soft tryptone agar) of the same strains was assayed at 37ºC for 4-6 hours.

722 **c**. Whole cell (cell) and supernatant (sec) proteins from late exponential-phase
723 cultures of a *Salmonella flgD* null strain expressing wild type FlgD (FlgD), a FlgD
724 variant in which residues 9-32 were replaced by two repeats of a six-residue
725 sequence Gly-Ser-Thr-Asn-Ala-Ser (labelled as 2xRpt) or its variants containing
726 between one and five additional residues inserted directly after the two repeats
727 (2xRpt+1, 2xRpt+2, 2xRpt+3, 2xRpt+4 or 2xRpt+5) were separated by SDS (15%)-
728 PAGE and analysed by immunoblotting with anti-FlgD polyclonal antisera. Swimming
729 motility (bottom panel; 0.25% soft tryptone agar) of the same strains was assayed at
730 37ºC for 4-6 hours.

731 **d**. Whole cell (cell) and supernatant (sec) proteins from late exponential-phase
732 cultures of a *Salmonella flgD* null strain expressing wild type FlgD (FlgD), a FlgD
733 variant in which residues 9-32 were replaced by two repeats of a six-residue
734 sequence Gly-Ser-Thr-Asn-Ala-Ser ($FlgD_{short}$) or suppressor mutants isolated from
735 this strain (rev1, rev2 or rev3) were separated by SDS (15%)-PAGE and analysed by
736 immunoblotting with anti-FlgD polyclonal antisera. Swimming motility (bottom panel;
737 0.25% soft tryptone agar) of the same strains were was assayed at 37ºC for 4-6
738 hours.

739 **e**. N-terminal sequences of wild type FlgD, a FlgD variant in which residues 9-32 are
740 replaced by two repeats of a six-residue sequence Gly-Ser-Thr-Asn-Ala-Ser (yellow;
741 $FlgD_{short}$) and its suppressor mutant revertants (rev 1-3) aligned at the gate
742 recognition motif (GRM, blue). Suppressor mutants contained insertions (underlined)
743 that introduced additional residues between the N-terminal hydrophobic signal
744 (orange) and the gate recognition motif (blue).

745

746 **Figure 3. Effect of the relative position of the N-terminus and GRM on the**

747 **export of rod and hook subunits**

748 **a.** Schematic representation of a wild type subunit (subunit$_{wild\ type}$), a subunit

749 containing a deletion of sequence between the N-terminus and GRM (subunit$_{short}$)

750 and a subunit in which the deleted sequence was replaced by four repeats of a six-

751 residue sequence Gly-Ser-Thr-Asn-Ala-Ser (yellow, subunit$_{short}$+4Rpt).

752 **b**. Whole cell (cell) and supernatant (sec) proteins from late exponential-phase

753 cultures of a *Salmonella flgE* null strain expressing wild type FlgG (FlgG$_{wild\ type}$), a

754 FlgG variant in which residues 11-35 were deleted (FlgG$_{short}$) or a FlgG variant in

755 which residues 11-35 were replaced by four repeats of a six-residue sequence Gly-

756 Ser-Thr-Asn-Ala-Ser (FlgG$_{short}$+4Rpt). All FlgG variants were engineered to contain

757 an internal 3xFLAG tag for immunodetection. Proteins were separated by SDS

758 (15%)-PAGE and analysed by immunoblotting with anti-FLAG monoclonal antisera.

759 Swimming motility (bottom panel; 0.25% soft tryptone agar) of the same strains was

760 assayed at 37ºC for 4-6 hours.

761 **c**. Whole cell (cell) and supernatant (sec) proteins from late exponential-phase

762 cultures of a *Salmonella flgD* null strain expressing wild type FlgE (FlgE$_{wild\ type}$), a

763 FlgE variant in which residues 9-32 were deleted (FlgE$_{short}$) or a FlgE variant in which

764 residues 9-32 were replaced by four repeats of a six-residue sequence Gly-Ser-Thr-

765 Asn-Ala-Ser (FlgE$_{short}$+4Rpt). All FlgE variants were engineered to contain an

766 internal 3xFLAG tag for immunodetection. Proteins were separated by SDS (15%)-

767 PAGE and analysed by immunoblotting with anti-FLAG monoclonal antisera.
768 Swimming motility (bottom panel; 0.25% soft tryptone agar) of the same strains was
769 assayed at 37ºC for 4-6 hours.

770 **Figure 4. Effect on subunit export of overexpression of FlgDΔ2-5 and variants.**

771 **a.** Schematic representation of a FlgD subunit containing a N-terminal hydrophobic
772 signal (orange, 2-5) and a gate-recognition motif (blue, GRM).

773 **b.** Swimming motility of a *Salmonella* Δ*recA* strain expressing wild type FlgD (FlgD),
774 its variants (DΔ2-5ΔGRM, DΔ2-5 or DΔGRM) or empty pTrc99a vector (-). Motility
775 was assessed in 0.25% soft-tryptone agar containing 100 µg/ml ampicillin and
776 100µM IPTG and incubated for 4-6 hours at 37°C.

777

778 **c.** Whole cell (cell) and secreted proteins (secreted) from late-exponential-phase
779 cultures were separated by SDS (15%)-PAGE and analysed by immunoblotting with
780 anti-FliK, anti-FlgK, anti-FlgL, anti-FlhA or anti-FlgN polyclonal antisera. Apparent
781 molecular weights are in kilodaltons (kDa).

782 **d**. A model depicting a FlgDΔ2-5 subunit (left) docked *via* its gate recognition motif
783 (GRM, blue) at the subunit binding pocket on $FlhB_C$ (PDB: 3B0Z[31], red), preventing
784 wild type subunits (right) from docking at $FlhB_C$.

785

786

787 **Figure 5. Effect on subunit export of overexpressed $FlgE_{short}$, $FlgD_{short}$ and**
788 **variants**

789 **a.** Swimming motility of a *Salmonella* Δ*recA* strain expressing wild type FlgE (FlgE
790 wild type), a FlgE variant in which residues 9-32 were deleted ($FlgE_{short}$), a FlgE
791 variant in which residues 9-32 and residues 39-43 (corresponding to the gate-
792 recognition motif) were deleted ($FlgE_{short}$ΔGRM), a FlgE variant in which residues
793 39-43 were deleted (FlgEΔGRM) or empty pTrc99a vector (-). All FlgG variants were
794 engineered to contain an internal 3xFLAG tag for immunodetection. Motility was
795 assessed in 0.25% soft-tryptone agar containing 100 µg/ml ampicillin and 100 µM
796 IPTG and incubated for 4-6 hours at 37°C (top panel). Whole cell (cell) and secreted
797 proteins (secreted) from late-exponential-phase cultures were separated by SDS
798 (15%)-PAGE and analysed by immunoblotting with anti-FLAG monoclonal antisera
799 or anti-FlgD, anti-FliD, anti-FlgK, anti-FliK, anti-FlhA or anti-FlgN polyclonal antisera
800 (bottom). Apparent molecular weights are in kilodaltons (kDa).

801 **b.** Swimming motility of a *Salmonella* Δ*recA* strain expressing wild type FlgD (FlgD
802 wild type), a FlgD variant in which residues 9-32 were replaced with two repeats of
803 the six amino acid sequence Gly-Ser-Thr-Asn-Ala-Ser ($FlgD_{short}$), a FlgD variant in
804 which residues 9-32 were replaced with two repeats of the six amino acid sequence
805 Gly-Ser-Thr-Asn-Ala-Ser and residues 36-40 were deleted ($FlgD_{short}$ΔGRM), a FlgD
806 variant in which residues 36-40 were deleted (FlgDΔGRM) or empty pTrc99a vector
807 (-). Motility was assessed in 0.25% soft-tryptone agar containing 100 µg/ml ampicillin
808 and 100 µM IPTG and incubated for 4-6 hours at 37°C (top panel). Whole cell (cell)
809 and secreted proteins (secreted) from late-exponential-phase cultures were

810 separated by SDS (15%)-PAGE and analysed by immunoblotting with anti-FlgD,
811 anti-FliD, anti-FlgK, anti-FliK, anti-FlhA or anti-FlgN polyclonal antisera (bottom).
812 Apparent molecular weights are in kilodaltons (kDa).

813 **Figure 6. Suppression of the $FlgD_{short}$ motility defect by mutations in FliP**

814 **a**. A model depicting subunits docked *via* their gate-recognition motif (GRM, blue) at
815 the subunit binding pocket on $FlhB_C$ (PDB: 3B0Z [31], red) with N-termini of early
816 flagellar subunits adopting either an α-helical conformation separating the N-terminal
817 hydrophobic signal (2-5, orange) and gate-recognition motif (GRM, blue) by ~40-60
818 Ångstrom (where each amino acid is on average separated by ~1.5Å, left) or an
819 unfolded conformation where the polypeptide contour length separating the N-
820 terminal hydrophobic signal (2-5) and gate-recognition motif (GRM) is ~90-150
821 Ångstrom (where each amino acid is on average separated by ~3.5Å, middle left).
822 Values corresponding to the distance separating the N-terminal hydrophobic signal
823 (2-5, orange) and gate-recognition motif (GRM, blue) of a FlgD subunit variant in
824 which residues 9-32 are replaced with two repeats of the six amino acid sequence
825 Gly-Ser-Thr-Asn-Ala-Ser ($FlgD_{short}$) indicate that the N-terminal hydrophobic signal
826 (2-5, orange) and gate-recognition motif (GRM, blue) are separated by ~29
827 Ångstrom (α-helical conformation, middle right) or ~67 Ångstrom (unfolded
828 polypeptide contour length, right).

829 **b.** Placement of the crystal structure of FlhBc (PDB:3BOZ [31]; red) and the cryo-EM
830 structure of FliPQR-FlhB (PDB:6S3L[30]) in a tomographic reconstruction of the
831 *Salmonella* SPI-1 injectisome (EMD-8544 [60]; grey). The minimum distance
832 between the subunit gate recognition motif binding site on $FlhB_C$ (grey) to $FlhB_N$

833 (defined as *Salmonella* FlhB residue 211 [62]; ~78Å) was estimated by combining:
834 the value corresponding to the distance between the subunit binding pocket on
835 $FlhB_C$ [14] (grey) and the N-terminal visible residue (D_{229}) in the $FlhB_C$ structure
836 (PDB:3BOZ [31]; ~52Å) with the value corresponding to the minimum distance
837 between FlhB residues 211 and 228 (based on a linear α-helical conformation;
838 ~26Å).

839

840 **c.** Swimming motility of recombinant *Salmonella flgD* null strains producing a
841 chromosomally-encoded FliP-M_{210}A variant (M_{210}A gate, left) or wild type FliP (wild
842 type gate, right). Wild type FliP and FliP-M_{210}A were engineered to contain an
843 internal HA tag positioned between residue 21 and 22 to allow immunodetection of
844 FliP. Both strains produced either a pTrc99a plasmid-encoded FlgD subunit variant
845 in which residues 9-32 were replaced with two repeats of the six amino acid
846 sequence Gly-Ser-Thr-Asn-Ala-Ser ($FlgD_{short}$; top panel) or a pTrc99a plasmid-
847 encoded wild type FlgD subunit ($FlgD_{wild\ type}$; bottom panel). Motility was assessed in
848 0.25% soft-tryptone agar containing 100 µg/ml ampicillin and 50 µM IPTG and
849 incubated for 16 hours (top panel) or 4-6 hours at 37°C (bottom panel).

850 **d.** The mean motility halo diameter of a recombinant *Salmonella flgD* null strain
851 producing chromosomally-encoded FliP-M_{210}A (M_{210}A gate, left) and expressing the
852 FlgD short variant (left hand bar) was plotted as a percentage of the mean motility
853 halo diameter of the wild type FliP gate strain (wild type) producing FlgDshort (right
854 hand bar). Error bars show the standard error of the mean calculated from four
855 biological replicates. * indicates a p-value < 0.05.

856 **Supplementary Figure Legends**

857 **Figure S1.**

858 **a**. N-terminal sequences of all *Salmonella* flagellar rod and hook subunits aligned at
859 their gate recognition motif (GRM, blue). Small non-polar residues upstream of the
860 gate recognition motif are highlighted (yellow).

861

862 **b**. Hydrophobicity plots for the N-terminal 60 residues of each *Salmonella* flagellar
863 rod and hook subunit were generated by ExPASy tools using the Kyte and Doolittle
864 method [62]. The *x* axis of the plot indicates the amino acid position, starting from the
865 N terminus. The *y* axis of the plot indicates the hydrophobicity of the amino acid
866 sequence, where higher values represent higher hydrophobicity. Amino acid
867 sequence corresponding to the gate-recognition motif of each subunit is highlighted
868 in blue.

869

870 **Figure S2**

871 **a**. Swimming motility of a *Salmonella* Δ*recA* strain expressing suppressor mutants
872 isolated from the FlgDΔ2-5 variant (FlgDΔ2-5 N_8I or FlgDΔ2-5 T_{11}I), the parent
873 FlgDΔ2-5 variant (DΔ2-5) or wild type FlgD (FlgD). Motility was assessed in 0.25%
874 soft-tryptone agar containing 100 µg/ml ampicillin and 50 µM IPTG and incubated 4-
875 6 hours at 37°C.

876

877 **b**. Swimming motility of a *Salmonella* Δ*recA* strain expressing wild type FlgD (FlgD),
878 FlgDΔ2-5 (DΔ2-5) or its variants containing a six-residue insertion between residues
879 19 and 20 of either small non-polar (AGAGAG) residues (DΔ2-5 3x(AG)), polar

880 (STSTST) residues (DΔ2-5 3x(ST)), or the sequence from an isolated insertion
881 suppressor mutant (GSGSMT) (DΔ2-5 GSGSMT). Motility was assessed in 0.25%
882 soft-tryptone agar containing 100 µg/ml ampicillin and 50 µM IPTG and incubated 4-
883 6 hours at 37°C.
884
885 **Figure S3**
886 **a**. Whole cell (cell) and supernatant (secreted) proteins from late exponential-phase
887 cultures of *Salmonella flgD* null strains expressing: suppressor mutants isolated from
888 the FlgDΔ2-5 variant (FlgDΔ2-5 N_8I or FlgDΔ2-5 T_{11}I), FlgDΔ2-5 variant (-) or wild
889 type FlgD (FlgD) were separated by SDS (15%)-PAGE and analysed by
890 immunoblotting with anti-FlhA or FlgN polyclonal antisera. Apparent molecular
891 weights are in kilodaltons (kDa).
892
893 **b**. Whole cell (cell) and supernatant (secreted) proteins from late exponential-phase
894 cultures of *Salmonella flgD* null strains expressing wild type FlgD (FlgD), FlgDΔ2-5
895 (DΔ2-5) or its variants containing a six-residue insertion between residues 19 and 20
896 of either small non-polar (AGAGAG) residues (DΔ2-5 3x(AG)), polar (STSTST)
897 residues (DΔ2-5 3x(ST)), or the sequence from an isolated insertion suppressor
898 mutant (GSGSMT) (DΔ2-5 GSGSMT) were separated by SDS (15%)-PAGE and
899 analysed by immunoblotting with anti-FlgD polyclonal antisera. Apparent molecular
900 weights are in kilodaltons (kDa).
901
902
903

904 **Figure S4**

905 **a**. Whole cell (cell) and supernatant (secreted) proteins from late exponential-phase
906 cultures of a *Salmonella flgD* null strain expressing suppressor mutants isolated from
907 a FlgDΔ2-5-^{19}(GSGSMT)^{20}-V_{15}A variant (V_{15}A-M_7I, V_{15}A-D_9A, V_{15}A-T_{11}I, V_{15}A-
908 G_{14}V), their parent FlgD variant FlgDΔ2-5-^{19}(GSGSMT)^{20}-V_{15}A (V_{15}A), FlgDΔ2-5-
909 ^{19}(GSGSMT)^{20} (-) or wild type FlgD (FlgD) were separated by SDS (15%)-PAGE
910 and analysed by immunoblotting with anti-FlhA and FlgN polyclonal antisera.
911 Apparent molecular weights are in kilodaltons (kDa).

912

913 **Figure S5**

914 **a**. Whole cell (cell) and supernatant (secreted) proteins from late exponential-phase
915 cultures of a *Salmonella flgD* null strain expressing wild type FlgD (FlgD), FlgDΔ9-32
916 or its variants in which residues 9-32 were replaced by between one and four six-
917 residue repeats of Gly-Ser-Thr-Asn-Ala-Ser (GSTNAS): (Δ9-32 4xRpt, Δ9-32 3xRpt,
918 Δ9-32 2xRpt, Δ9-32 1xRpt) were separated by SDS (15%)-PAGE and analysed by
919 immunoblotting with anti-FlhA and anti-FlgN polyclonal antisera. Apparent molecular
920 weights are in kilodaltons (kDa).

921

922 **b**. Whole cell (cell) and supernatant (secreted) proteins from late exponential-phase
923 cultures of a *Salmonella flgD* null strain expressing wild type FlgD (FlgD), a FlgD
924 variant in which residues 9-32 were replaced by two repeats of a six-residue
925 sequence Gly-Ser-Thr-Asn-Ala-Ser (2xRpt) or its variants containing between one
926 and five additional residues inserted directly after the two repeats (2xRpt+ 1, 2xRpt+
927 2, 2xRpt+ 3, 2xRpt+ 4 or 2xRpt+ 5) were separated by SDS (15%)-PAGE and

928 analysed by immunoblotting with anti-FlgD polyclonal antisera. Apparent molecular
929 weights are in kilodaltons (kDa).
930
931 **Figure S6**
932 **a**. Whole cell (cell) and supernatant (secreted) proteins from late exponential-phase
933 cultures of a *Salmonella flgD* null strain expressing wild type FlgD (FlgD), a FlgD
934 variant in which residues 9-32 were replaced by two repeats of a six-residue
935 sequence Gly-Ser-Thr-Asn-Ala-Ser ($FlgD_{short}$) or suppressor mutants isolated from
936 this strain (rev1, rev2 or rev3) were separated by SDS (15%)-PAGE and analysed by
937 immunoblotting with anti-FlhA and anti-FlgN polyclonal antisera. Apparent molecular
938 weights are in kilodaltons (kDa).
939
940 **b**. N-terminal sequences of wild type FlgD (wild type), a FlgD variant in which residus
941 9-32 are replaced by two repeats of a six-residue sequence Gly-Ser-Thr-Asn-Ala-Ser
942 (yellow; $FlgD_{short}$) and its suppressor mutants (rev 1-7) aligned to their gate-
943 recognition motif (GRM, blue). Suppressor mutants contained insertions (underlined)
944 that introduced additional residues between the N-terminal hydrophobic signal
945 (orange) and the gate-recognition motif (blue).
946
947 **Figure S7**
948 **a**. Whole cell (cell) and supernatant (sec) proteins from late exponential-phase
949 cultures of a *Salmonella flgE* null strain expressing wild type FlgG ($FlgG_{wild\ type}$), a
950 FlgG variant in which residues 11-35 were deleted ($FlgG_{short}$) or a FlgG variant in
951 which residues 11-35 were replaced by four repeats of a six-residue sequence Gly-

952 Ser-Thr-Asn-Ala-Ser ($FlgG_{short}$+4Rpt). All FlgG variants were engineered to contain
953 an internal 3xFLAG tag for immunodetection. Proteins were separated by SDS
954 (15%)-PAGE and analysed by immunoblotting with anti-FlhA or anti-FlgN polyclonal
955 antisera. Apparent molecular weights are in kilodaltons (kDa).
956
957 **b**. Whole cell (cell) and supernatant (secreted) proteins from late exponential-phase
958 cultures of a *Salmonella flgD* null strain expressing wild type FlgE ($FlgE_{wild\ type}$), a
959 FlgE variant in which residues 9-32 were deleted ($FlgE_{short}$) or a FlgE variant in which
960 residues 9-32 were replaced by four repeats of a six-residue sequence Gly-Ser-Thr-
961 Asn-Ala-Ser ($FlgE_{short}$+4Rpt). All FlgE variants were engineered to contain an
962 internal 3xFLAG tag for immunodetection. Proteins were separated by SDS (15%)-
963 PAGE and analysed by immunoblotting with anti-FLAG monoclonal antisera.
964 Swimming motility (bottom panel; 0.25% soft tryptone agar) of the same strains were
965 carried out at 37ºC for 4-6 hours. Apparent molecular weights are in kilodaltons
966 (kDa).
967
968 **Figure S8**
969 **a**. Whole cell (cell) proteins from late exponential-phase cultures of recombinant
970 *Salmonella flgD* null strains producing a chromosomally-encoded FliP-M_{210}A variant
971 (M_{210}A gate, left) or wild type FliP (wild type gate, right). Wild type FliP and FliP-
972 M_{210}A were engineered to contain an internal HA tag positioned between residue 21
973 and 22 to allow immunodetection of FliP [29] (bottom panel). Both strains produced
974 either a pTrc99a plasmid-encoded FlgD subunit variant in which residues 9-32 were
975 replaced with two repeats of the six amino acid sequence Gly-Ser-Thr-Asn-Ala-Ser

976 (FlgD$_{short}$; top panel) or a pTrc99a plasmid-encoded wild type FlgD subunit (FlgD$_{wild}$

977 $_{type}$; middle panel). Proteins were separated by SDS (15%)-PAGE and analysed by

978 immunoblotting with anti-FlgD polyclonal antisera or anti-HA monoclonal antisera.

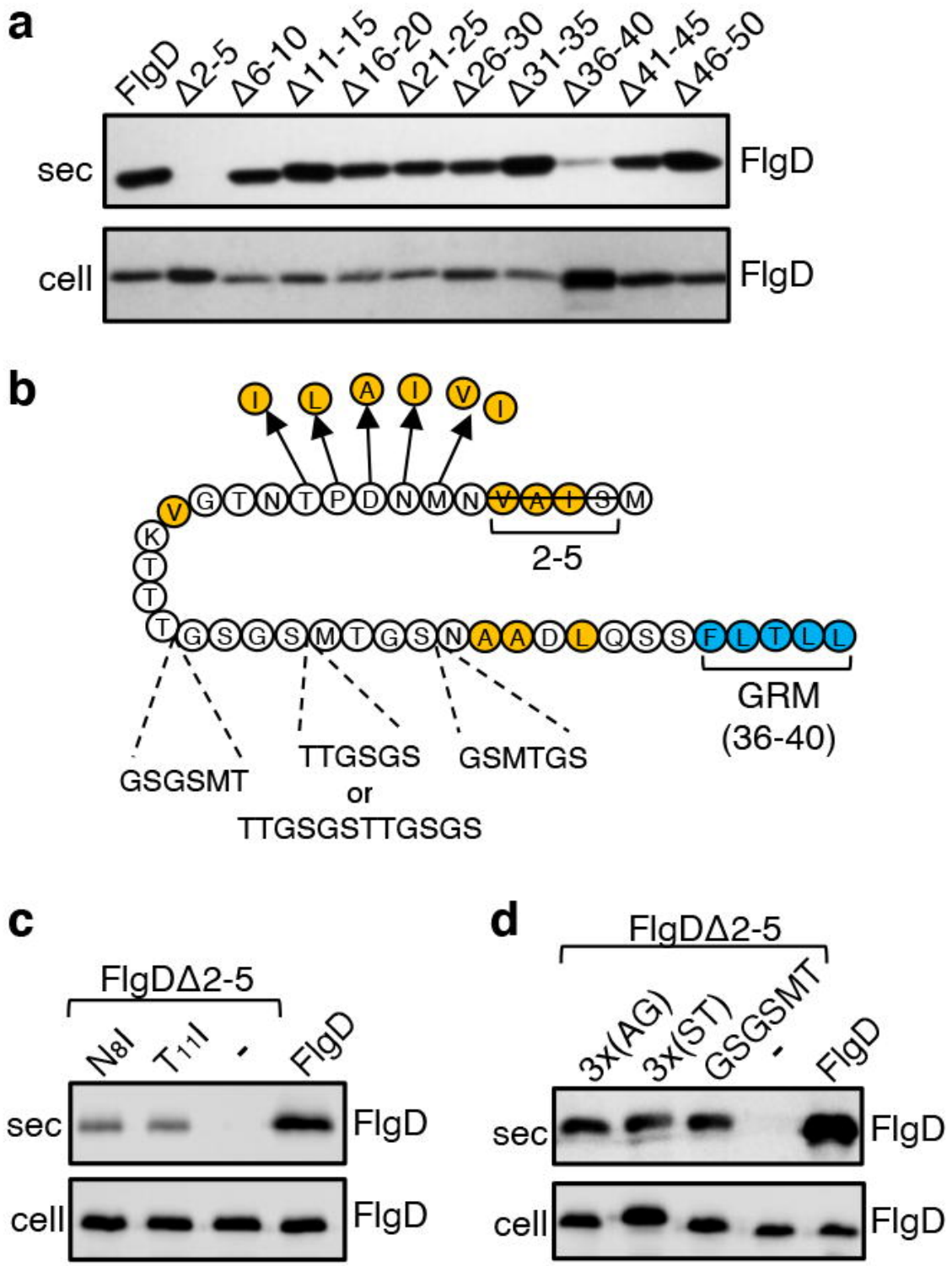
a
FlgD
Δ2-5
Δ6-10
Δ11-15
Δ16-20
Δ21-25
Δ26-30
Δ31-35
Δ36-40
Δ41-45
Δ46-50
sec
cell
FlgD
FlgD
b
I L A I V I
V G T N T P D N M N V A I S M
K T T T
T G S G S M T G S N A A D L Q S S F L T L L
2-5
GRM
(36-40)
GSGSMT
TTGSGS
or
TTGSGSTTGSGS
GSMTGS
c
FlgDΔ2-5
N8I
T11I
-
FlgD
sec
cell
FlgD
FlgD
d
FlgDΔ2-5
3x(AG)
3x(ST)
GSGSMT
-
FlgD
sec
cell
FlgD
FlgD

Figure 1

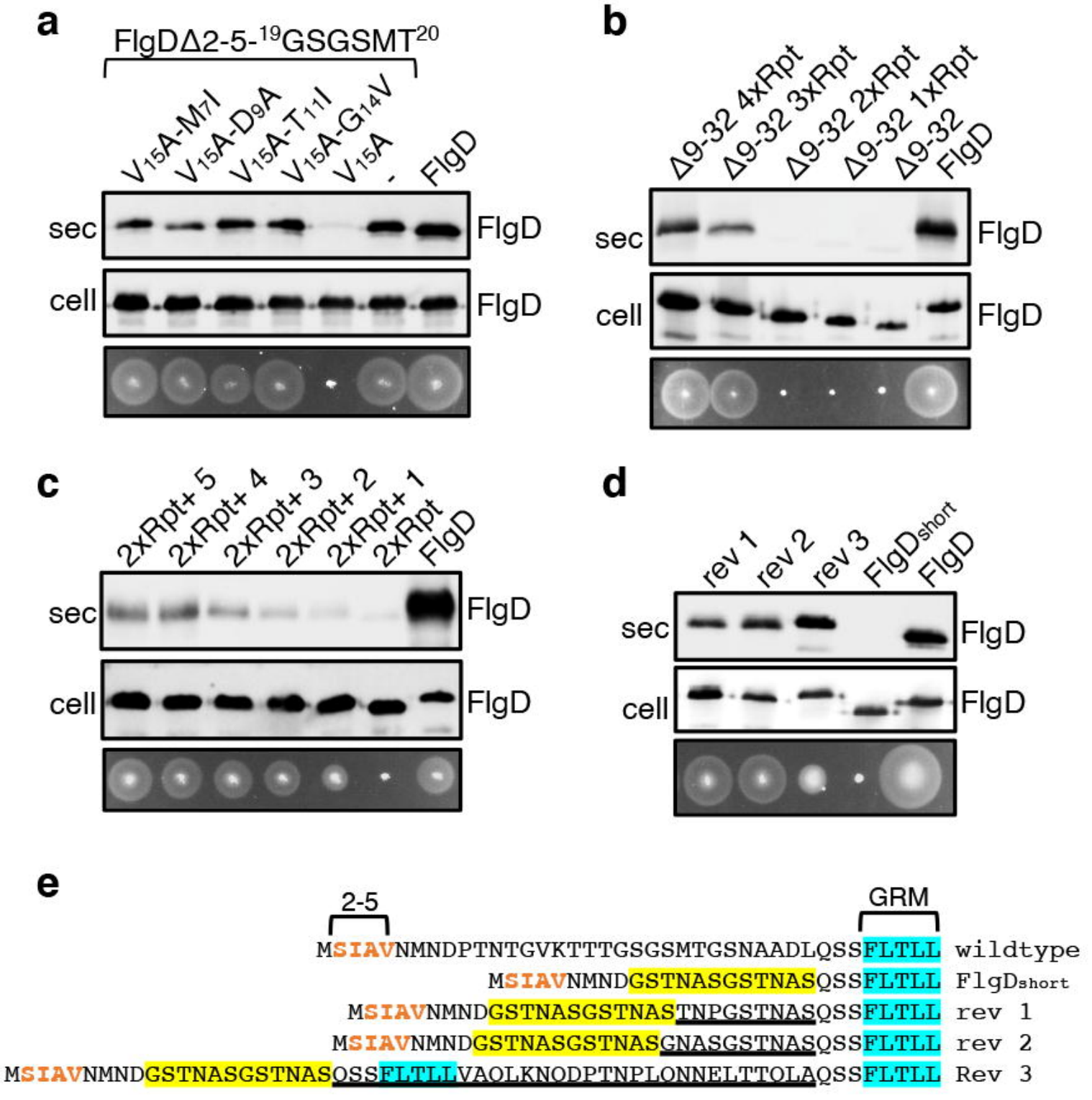
a
FlgDΔ2-5-19GSGSMT20
V15A-M7I
V15A-D9A
V15A-T11I
V15A-G14V
V15A
-
FlgD
sec
cell
FlgD
b
Δ9-32 4xRpt
Δ9-32 3xRpt
Δ9-32 2xRpt
Δ9-32 1xRpt
Δ9-32
FlgD
c
2xRpt+ 5
2xRpt+ 4
2xRpt+ 3
2xRpt+ 2
2xRpt+ 1
2xRpt
d
rev 1
rev 2
rev 3
FlgDshort
e
2-5
GRM
MSIAVNMNDPTNTGVKTTTGSGSMTGSNAADLQSSFLTLL wildtype
MSIAVNMNDGSTNASGSTNASQSSFLTLL FlgDshort
MSIAVNMNDGSTNASGSTNASTNPGSTNASQSSFLTLL rev 1
MSIAVNMNDGSTNASGSTNASGNASGSTNASQSSFLTLL rev 2
MSIAVNMNDGSTNASGSTNASQSSFLTLLVAQLKNQDPTNPLQNNELTTQLAQSSFLTLL Rev 3

Figure 2

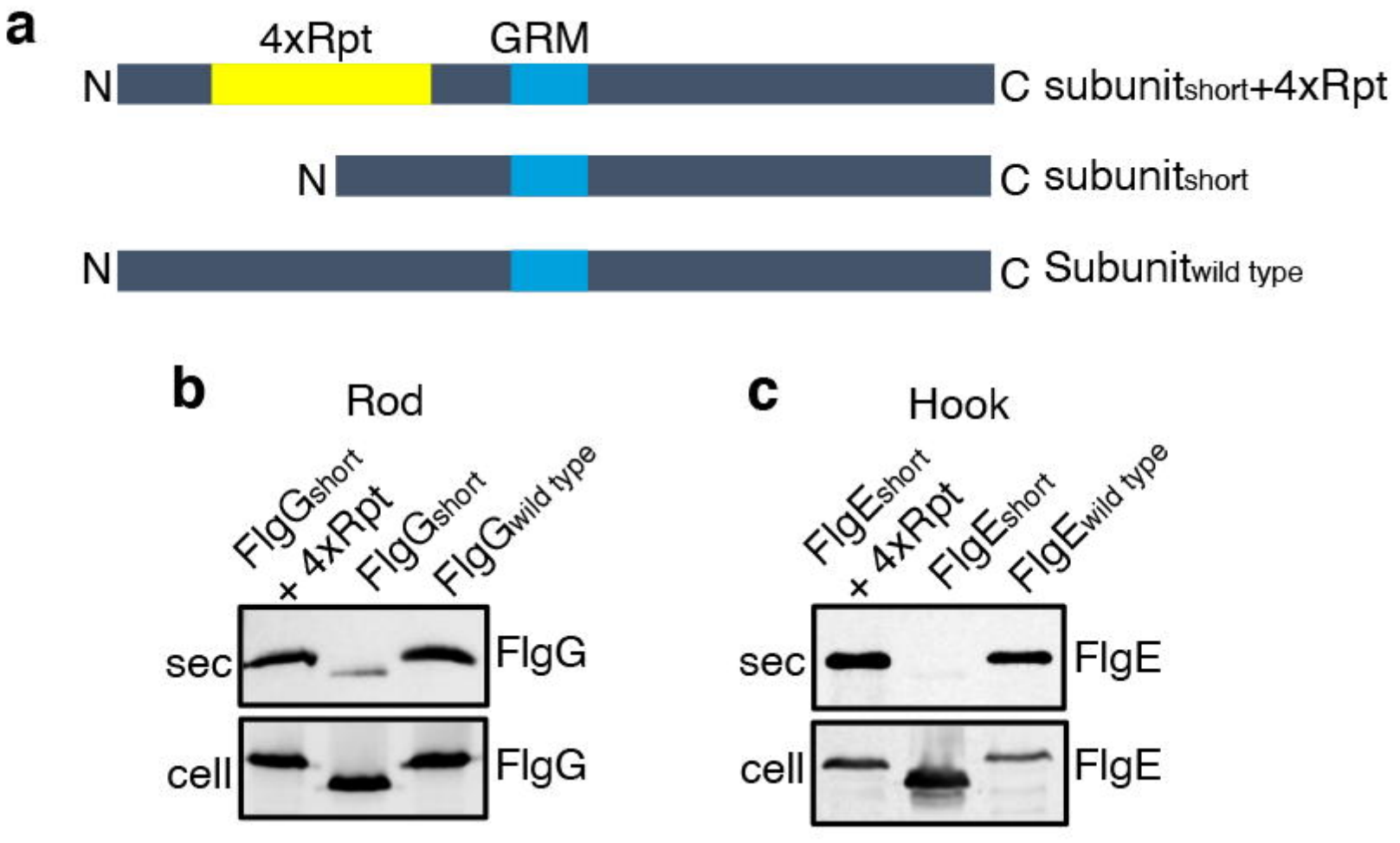
a
4xRpt
GRM
N
C subunitshort+4xRpt
N
C subunitshort
N
C Subunitwild type
b
Rod
FlgGshort + 4xRpt
FlgGshort
FlgGwild type
sec
cell
FlgG
FlgG
c
Hook
FlgEshort + 4xRpt
FlgEshort
FlgEwild type
sec
cell
FlgE
FlgE

Figure 3

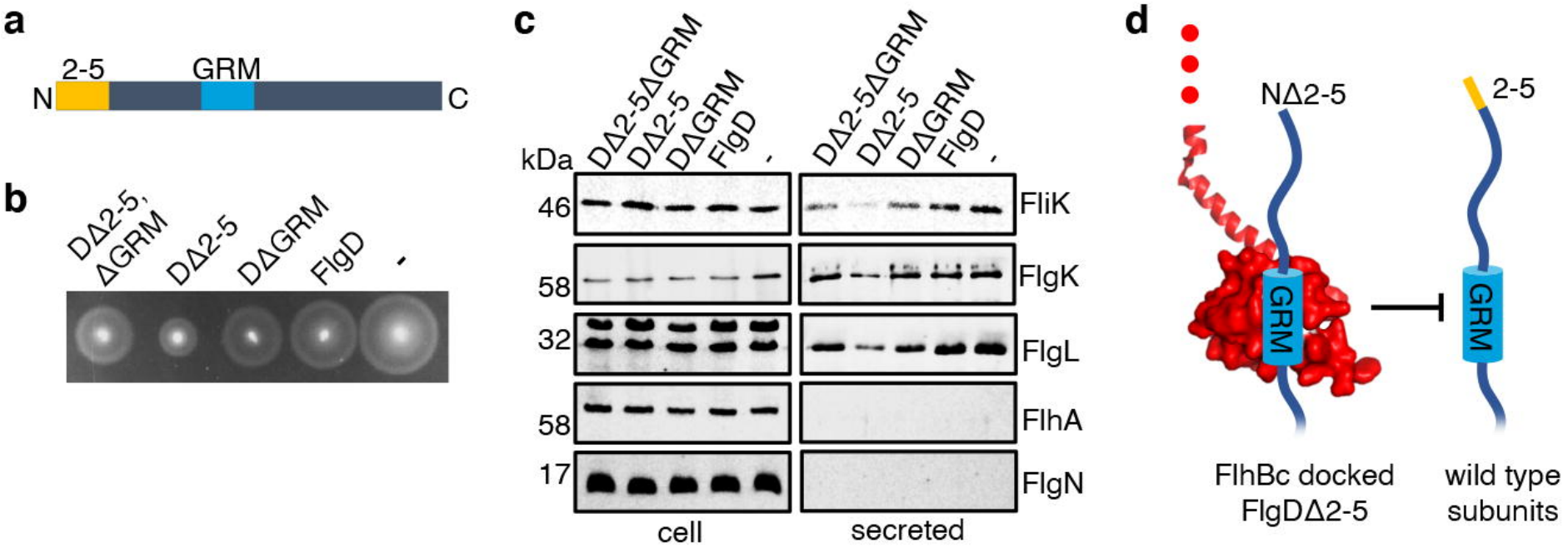
a
2-5
GRM
N
C
b
DΔ2-5, ΔGRM
DΔ2-5
DΔGRM
FlgD
-
c
kDa
DΔ2-5ΔGRM
DΔ2-5
DΔGRM
FlgD
-
46
58
32
58
17
FliK
FlgK
FlgL
FlhA
FlgN
cell
secreted
d
NΔ2-5
2-5
GRM
GRM
FlhBc docked FlgDΔ2-5
wild type subunits

Figure 4

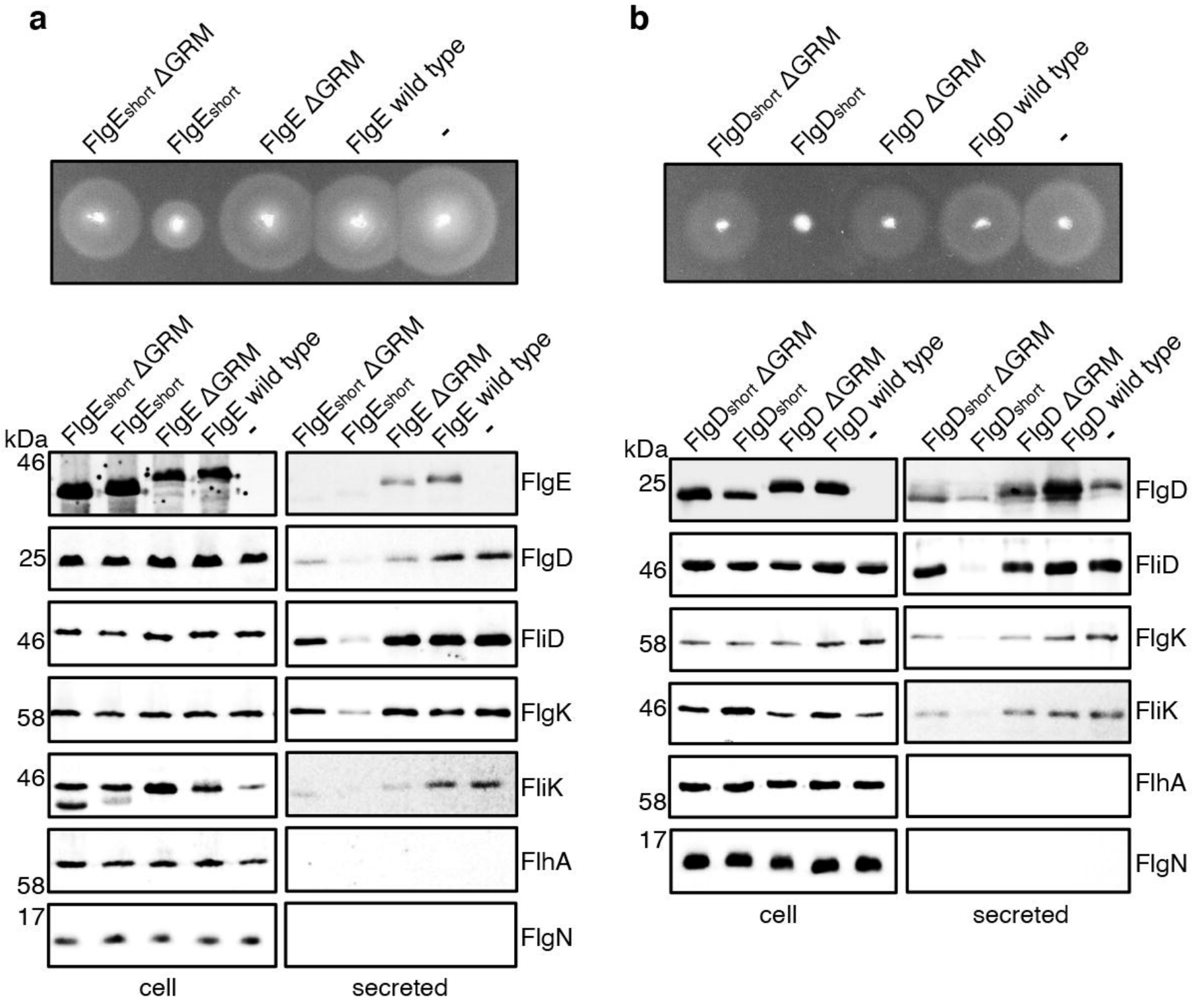
a
FlgEshort ΔGRM
FlgEshort
FlgE ΔGRM
FlgE wild type
-
kDa
46
25
46
58
46
58
17
FlgE
FlgD
FliD
FlgK
FliK
FlhA
FlgN
cell
secreted
b
FlgDshort ΔGRM
FlgDshort
FlgD ΔGRM
FlgD wild type
-
kDa
25
46
58
46
58
17
FlgD
FliD
FlgK
FliK
FlhA
FlgN
cell
secreted

Figure 5

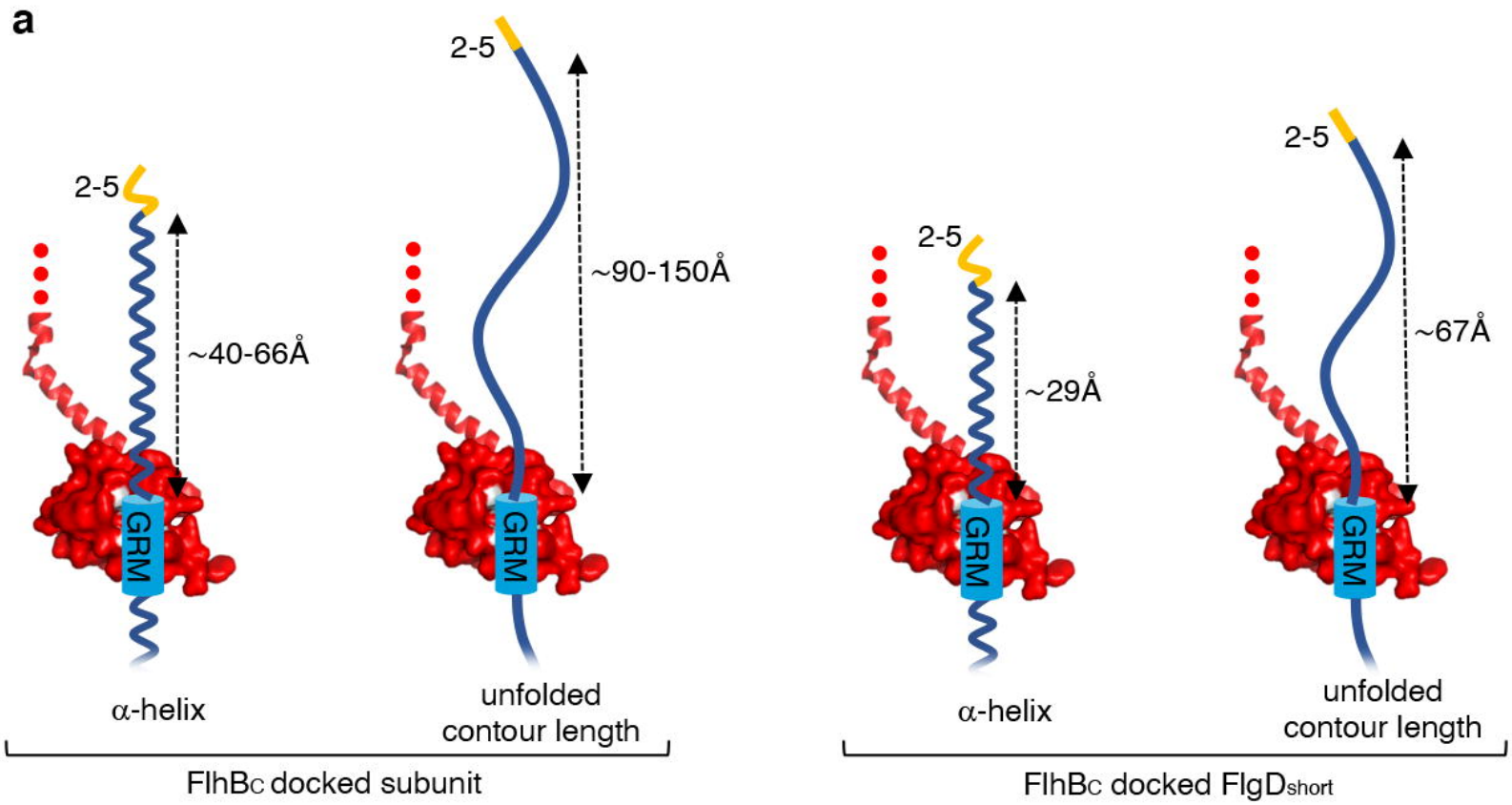
a
2-5
~40-66Å
GRM
α-helix
2-5
~90-150Å
GRM
unfolded
contour length
FlhBc docked subunit
2-5
~29Å
GRM
α-helix
2-5
~67Å
GRM
unfolded
contour length
FlhBc docked FlgDshort

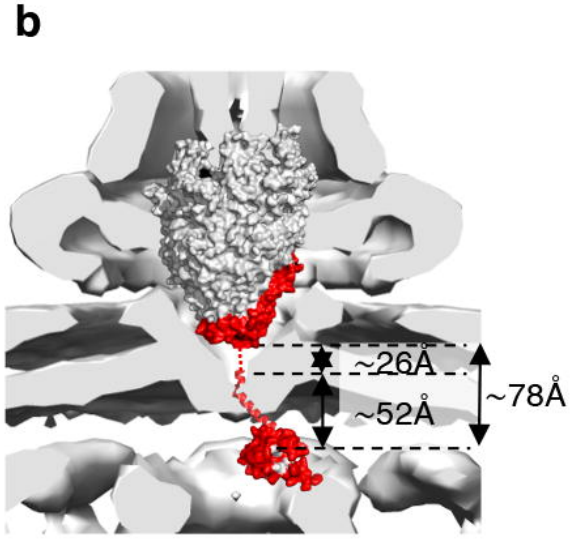
b
~26Å
~52Å
~78Å

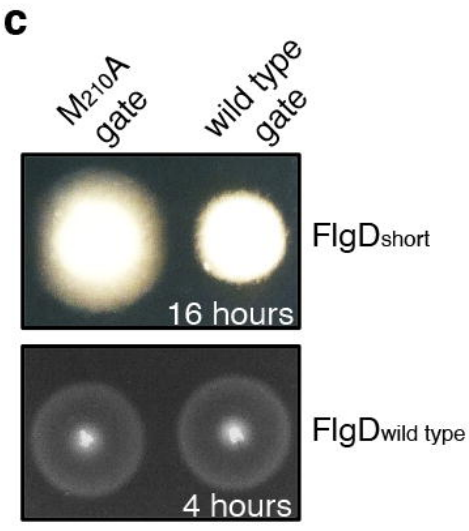
c
M210A gate
wild type gate
FlgDshort
16 hours
FlgDwild type
4 hours

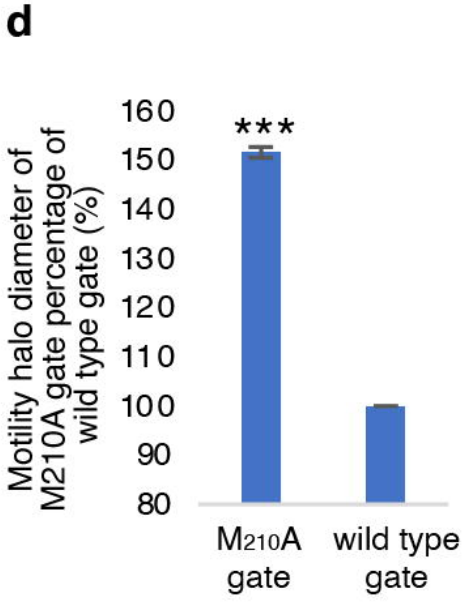
d
Motility halo diameter of M210A gate percentage of wild type gate (%)
160
150
140
130
120
110
100
90
80
***
M210A gate
wild type gate

Figure 6